CrystEngComm

Accepted Manuscript

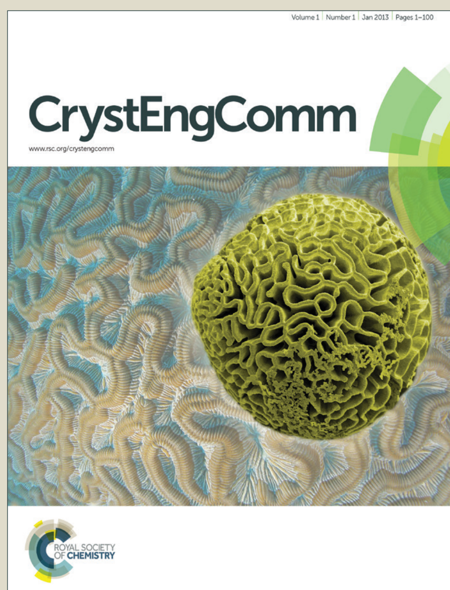

This is an *Accepted Manuscript*, which has been through the Royal Society of Chemistry peer review process and has been accepted for publication.

Accepted Manuscripts are published online shortly after acceptance, before technical editing, formatting and proof reading. Using this free service, authors can make their results available to the community, in citable form, before we publish the edited article. We will replace this *Accepted Manuscript* with the edited and formatted *Advance Article* as soon as it is available.

You can find more information about *Accepted Manuscripts* in the Information for Authors.

Please note that technical editing may introduce minor changes to the text and/or graphics, which may alter content. The journal's standard Terms & Conditions and the Ethical guidelines still apply. In no event shall the Royal Society of Chemistry be held responsible for any errors or omissions in this *Accepted Manuscript* or any consequences arising from the use of any information it contains.

ROYAL SOCIETY OF CHEMISTRY

www.rsc.org/crystengcomm

Strain relaxation of the $In_{0.53}Ga_{0.47}As$ epi-layer grown on Si substrate by molecular beam epitaxy

Fangliang Gao[a], Lei Wen[a], Yunfang Guan[a], Jingling Li[a], Xiaona Zhang[b], Miaomiao Jia[b], Shuguang Zhang[*a] and Guoqiang Li[*a]

[a]*State Key Laboratory of Luminescent Materials and Devices, South China University of Technology, Guangzhou, 510641, China*
[b]*Institute of Microstructure and Properties of Advanced Materials, Beijing University of Technology, Beijing, 100022, China*

[*]Author to whom correspondence should be addressed. Electronic mail: mssgzhang@scut.edu.cn, msgli@scut.edu.cn

Abstract: The $In_{0.53}Ga_{0.47}As$ films were grown on the Si (111) substrate with two different $In_xGa_{1-x}As$ buffer layers by molecular beam epitaxy (MBE). The effect of buffer layer on the as-grown $In_{0.53}Ga_{0.47}As$ epi-layers was investigated by X-ray diffraction (XRD), reciprocal space mapping (RSM), Raman and transmission electron microscopy (TEM). XRD results showed that the crystalline quality of as-grown $In_{0.53}Ga_{0.47}As$ epi-layer grown on Si substrate by using low-temperature $In_{0.4}Ga_{0.6}As$ buffer layer with in-situ annealing was better than that by using $In_{0.2}Ga_{0.8}As/In_{0.4}Ga_{0.6}As$ buffer layers. Moreover, the misfit strain between $In_{0.53}Ga_{0.47}As$ epi-layers and Si substrate was nearly completely released by inserting a single $In_{0.4}Ga_{0.6}As$ buffer layer grown at 390 °C with in-situ annealing at 560 °C. Specifically, the relaxation value of the $In_{0.53}Ga_{0.47}As$ epi-layer with the single $In_{0.4}Ga_{0.6}As$ buffer layer was 97.16 %. The lattice mismatch strain of the $In_{0.53}Ga_{0.47}As$ epi-layer was well confined to the $In_{0.4}Ga_{0.6}As$ buffer layer, without extended to the subsequently grown $In_{0.53}Ga_{0.47}As$ epi-layer compared with its counterpart using the $In_{0.2}Ga_{0.8}As/In_{0.4}Ga_{0.6}As$ buffer layers. The low-temperature $In_{0.4}Ga_{0.6}As$ buffer layer shows a way to realize high crystalline quality and fully relaxed $In_{0.53}Ga_{0.47}As$ films on the Si substrate.

Key words: $In_{0.53}Ga_{0.47}As$, stress relaxation, dislocation, molecular beam epitaxy

1. Introductions

The heteroepitaxy of $In_xGa_{1-x}As$ films on various types of substrates is widely used in many advanced electronic and optoelectronic applications, mainly for the following two reasons. Firstly, the energy band gap (E_g) of $In_xGa_{1-x}As$ material covers the range from 0.36 (InAs) to 1.42 eV (GaAs) which is suitable for high-efficiency solar cells,[1] laser diodes,[2] photodetectors,[3-5] and so on. Moreover, the $In_xGa_{1-x}As$ material has high carrier mobility which is essential for high-speed electronic devices.[6, 7] In particular, $In_{0.53}Ga_{0.47}As$ is an ideal III-V compound semiconductor for a metal-oxide-semiconductor field-effect transistor (MOSFET) channel material due

CrystEngComm Accepted Manuscript

to its high electronic mobility and high breakdown field.[8] However, the performance of the device is mainly influenced by the crystalline quality of $In_{0.53}Ga_{0.47}As$. Therefore, improving the crystalline quality is a key issue for high-performance III-V MOSFET. In general, the InP and GaAs are most commonly used as substrates for the growth of $In_{0.53}Ga_{0.47}As$ due to the lattice matching between them. Unfortunately, the InP and GaAs substrates have their disadvantages such as high cost, small size and large brittleness.[9] Undoubtly, the Si wafers are most widely utilized as the substrates in the micro-electronics and large scale integrated circuits, and about 95 % of all semiconductor devices are presently fabricated using Si. A Si wafer as the carrier, is considerably advantageous due to its higher thermal conductivity, low cost, large size and very mature process technology.[10-12] Therefore, the researchers considered using Si as an alternative for the epitaxy of $In_{0.53}Ga_{0.47}As$ film. However, the intrinsic strain typically arises due to the constraint of heteroepitaxy considering the different lattice parameters between the epi-film and the substrate. If $In_{0.53}Ga_{0.47}As$ is directly grown on Si, a great number of defects will be generated in the as-grown $In_{0.53}Ga_{0.47}As$ film due to the large lattice mismatch, ultimately leading to a deteriorated device performance.[13] In order to obtain better relaxation and high-quality $In_{0.53}Ga_{0.47}As$ epitaxial films on the Si substrate, one effective way is to use buffer layers to reduce the stress caused by lattice mismatch between them. Therefore, the structure and epitaxial growth procedures of buffer layers are of paramount importance to achieve high-quality $In_{0.53}Ga_{0.47}As$ films on Si.

In this work, we report on the growth of $In_{0.53}Ga_{0.47}As$ epitaxial films on 2-inch Si (111) substrate by molecular beam epitaxy (MBE) using composition-graded $In_{0.2}Ga_{0.8}As/In_{0.4}Ga_{0.6}As$ buffer layers and a single $In_{0.4}Ga_{0.6}As$ buffer layer, respectively. Two samples using these two different buffer layers were grown to compare the strain relaxation. The investigation results showed that the buffer layers have great effect on the strain relaxation during the heteroepitaxy. The better relaxation $In_{0.53}Ga_{0.47}As$ epi-layer is the one grown on the $In_{0.4}Ga_{0.6}As$ single buffer layer with a low growth temperature and in-situ annealing. This achievement is of great interest for a simple approach to achieve high-quality $In_{0.53}Ga_{0.47}As$ films on the Si substrates.

2. Experimental details

The $In_{0.53}Ga_{0.47}As$ films were grown on 2-inch diameter Si (111) substrates by MBE. High purity In (7N), Ga (7N) and As (7N) were used as the sources, respectively. The Si substrates were primarily ultrasonically cleaned with chemicals and deionized water to remove the surface contaminations and finally dried by 7N nitrogen gas before being put into the MBE load-lock chamber with a pressure of 3.2×10^{-7} Torr. The substrates were then transferred into the high-vacuum MBE growth chamber under a pressure of 4.0×10^{-10} Torr and annealed at 1000 °C for 30 min to remove the surface oxidized layer. Two samples were grown using buffer layers of different structures. For sample A, the composition-graded $In_{0.2}Ga_{0.8}As/In_{0.4}Ga_{0.6}As$ buffer layers were utilized for the epitaxy of $In_{0.53}Ga_{0.47}As$. Each sub-layer thickness of buffer layer was ~ 6 nm and the growth temperature was remained at 560 °C. The

CrystEngComm Accepted Manuscript

composition-graded $In_{0.2}Ga_{0.8}As/In_{0.4}Ga_{0.6}As$ buffer layers of 12 nm were grown in total thickness. In order to study the effect of the buffer layer on the $In_{0.53}Ga_{0.47}As$ film crystalline quality, the buffer layer was grown at a low temperature for comparison. For sample B, a single $In_{0.4}Ga_{0.6}As$ buffer layer of 12 nm was grown before the subsequent epitaxy of the $In_{0.53}Ga_{0.47}As$ film. The growth temperature of buffer layer was 390 °C with a 5 min in-situ post-annealing at 560 °C. The substrate temperature was then fixed to 560 °C and a 100 nm thick $In_{0.53}Ga_{0.47}As$ layer was grown afterwards for both samples. The crystallinity of as-grown films were characterized by high-resolution X-ray diffraction (XRD) with Cu $K\alpha_1$ as the X-ray source (Bruker D8 Discover). Raman spectra was obtained at room temperature using 514.5-nm line of Ar^+ laser as an exciting source. Transmission electron microscopy (TEM, JEOL 3000F) was carried out to study the microstructure of the samples. The field emission gun of TEM was working at a voltage of 300 kV, which gave a point to point resolution of 0.17 nm.

3. Results and discussions

The structural properties of as-grown $In_{0.53}Ga_{0.47}As$ films on Si (111) substrate were investigated by XRD. Fig. 1(a) shows the typical XRD patterns of sample A. We have confirmed the $In_{0.53}Ga_{0.47}As$ epi-layers from diffraction angle. Except for the diffraction peaks from $In_{0.53}Ga_{0.47}As$ (111) and the Si (111) substrate, no other diffraction peaks are detected, which confirms that the $In_{0.53}Ga_{0.47}As$ epi-layer is single crystalline. The influence of buffer layer on the crystalline quality of as-grown $In_{0.53}Ga_{0.47}As$ epi-layers is studied by X-ray rocking curves (XRCs). Fig. 1(b) represents the XRCs for $In_{0.53}Ga_{0.47}As$ epi-layers (111) grown on Si (111) substrates using two different buffer layers, from which the crystalline quality of as-grown $In_{0.53}Ga_{0.47}As$ could be evaluated. The full-width at half-maximums (FWHMs) are about 595.56 and 556.41 arcsec for as-grown $In_{0.53}Ga_{0.47}As$ epi-layers with the sample A and B, respectively. Apparently, $In_{0.53}Ga_{0.47}As$ grown on Si (111) with the low-temperature and in-situ annealing $In_{0.4}Ga_{0.6}As$ buffer layer exhibits higher crystallinity than that grown with composition-graded buffer layers.

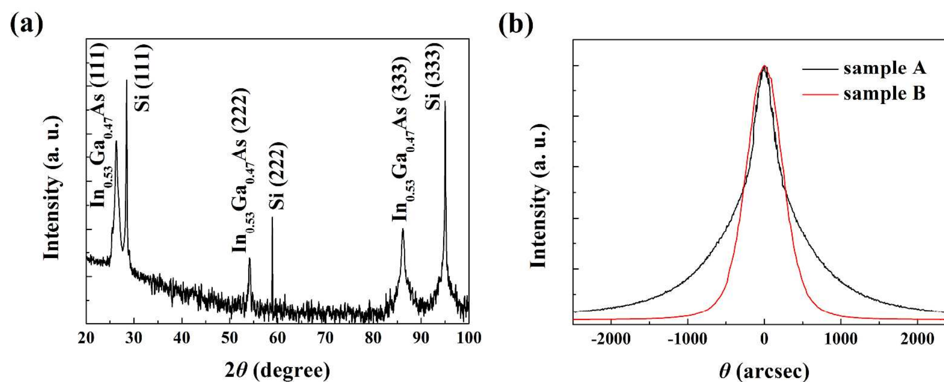

Fig. 1(a) Typical XRD analysis of sample A using composition-graded buffer layers, (b) XRCs of as-grown $In_{0.53}Ga_{0.47}As$ (111) planes for sample A and B, respectively.

CrystEngComm Accepted Manuscript

In order to study the strain state of the epitaxial $In_{0.53}Ga_{0.47}As$ films, reciprocal space mappings (RSMs) measurement was carried out for both the symmetric (111) and asymmetric (224) planes of the 100 nm thick $In_{0.53}Ga_{0.47}As$ films, as shown in Fig. 2. The reciprocal space coordinates in this paper are denoted as (q_x, q_z) which are transformed from the real space angles.

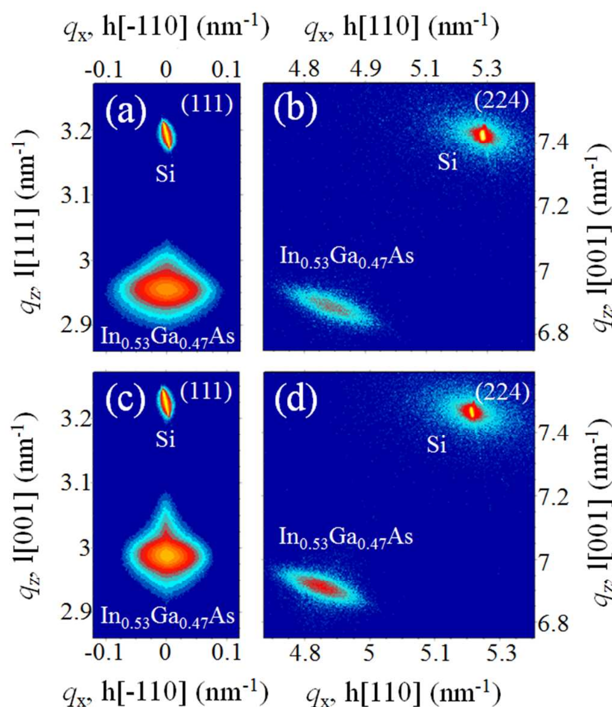

Fig. 2 The RSMs of $In_{0.53}Ga_{0.47}As$ films grown on Si using two different buffer layers for sample A (a, b) and sample B (c, d), respectively.

Fig. 2(a)-(b) present RSMs results of sample A for the diffraction plane of (111) and (224), respectively. It is distinctly observed from Fig. 2(a) that the $In_{0.53}Ga_{0.47}As$ (111) layer are sitting rightly behind Si (111) substrate in the reciprocal space, indicating the epitaxial relationship of $In_{0.53}Ga_{0.47}As$ (111) || Si (111). Besides, the diffraction patterns of the Si (111) substrate and the $In_{0.53}Ga_{0.47}As$ epitaxial layer are well resolved. The $In_{0.53}Ga_{0.47}As$ film displays an elliptically shaped diffraction pattern, which can be attributed to the mosaic structure of the epi-layer, crystallographic tilt of the epi-layer, and the crystalline distortion.[14] Fig. 2(b) shows the asymmetric (224) RSM of the samples A with the composition-graded buffers. We can clearly observe that the diffraction peaks of $In_{0.53}Ga_{0.47}As$ (224) presents an obvious broadening along the mosaic direction.[15] The (111) RSM of sample B in Fig. 2(c) also reveals the epitaxial relationship of $In_{0.53}Ga_{0.47}As$ (111) || Si (111). However, the (111) RSM diffraction pattern of the $In_{0.53}Ga_{0.47}As$ film displays an approximately circle shape, which manifests an improved crystalline quality of the $In_{0.53}Ga_{0.47}As$ films using a single $In_{0.4}Ga_{0.6}As$ buffer layer. The asymmetric (224) RSM of the sample B are shown in Fig. 2(d), which also exhibits a broaden elliptical shape along

CrystEngComm Accepted Manuscript

the mosaic direction. It has been reported that broadening of the peak in various directions is due to the crystal imperfections. Diffraction peak broadening along the mosaic direction was an indication of the presence of mosaic blocks which slightly rotate the allowable diffraction plane in their vicinity.[15]

In order to further verify the relaxation state of the as-grown $In_{0.53}Ga_{0.47}As$ films, we have calculated the relaxation value of the $In_{0.53}Ga_{0.47}As$ epi-layers. As we know, the lattice constant of $In_xGa_{1-x}As$ ($0<x<1$, $5.6533<a<6.0584$ Å) material is larger than that of Si (a = 5.4310 Å) which results in compressively strained as-grown $In_{0.53}Ga_{0.47}As$ film. The relaxed lattice constants of the epitaxial layer are then calculated by assuming a linear interpolation (Vegard's law) between the lattice constants of the binary alloy constituents (GaAs and InAs).[16] The lattice constant and the misfit strain to Si substrate for $In_xGa_{1-x}As$ employed in this work as shown in Table 1.[17] Therefore, the lattice parameter of the fully relaxed $In_{0.53}Ga_{0.47}As$ epi-layer can be calculated to be a_0^{l} = 5.8680 Å. On the other hand, the lattice parameter of the $In_{0.53}Ga_{0.47}As$ epi-layers can be derived according to the RSM results.[18] Therefore, the lattice parameter of as-grown $In_{0.53}Ga_{0.47}As$ films for samples A and B are a^{l} = 5.8206±0.0047 and 5.8470±0.0086 Å, respectively. Additionally, the layer relaxation value R, can be defined by:[14]

$$R = \frac{a^{\mathrm{l}} - a_0^{\mathrm{s}}}{a_0^{\mathrm{l}} - a_0^{\mathrm{s}}} \quad (1)$$

where a^{l} is the strained layer lattice parameter, and a_0^{s} and a_0^{l} are the fully relaxed lattice parameters of substrate and epi-layer, respectively. Thus, the relaxation values of the $In_{0.53}Ga_{0.47}As$ epi-layers for sample A and B are R = 89.15±1.08 % and 95.19±1.97 %, respectively. This result indicated that the better relaxation $In_{0.53}Ga_{0.47}As$ epi-layer was grown on the $In_{0.4}Ga_{0.6}As$ single buffer layer with a low growth temperature and in-situ annealing, compared to the sample A with the composition-graded buffer layers.

Table 1 Lattice constant and the misfit strain between the Si and $In_xGa_{1-x}As$ employed materials in this work.

Material	Lattice constant (Å)	Misfit (%)
Si	5.4310	0
GaAs	5.6533	4.09
InAs	6.0584	11.55
$In_{0.2}Ga_{0.8}As$	5.7343	5.58
$In_{0.4}Ga_{0.6}As$	5.8153	7.08
$In_{0.53}Ga_{0.47}As$	5.8680	8.05

Fig. 3 shows Raman spectra from the samples with two different buffer layers. The first order Raman spectrum of a semiconductor typically reveal the longitudinal optical (LO) and transversal optical (TO) phonons information.[19] However, the

CrystEngComm Accepted Manuscript

ternary compound semiconductor $In_xGa_{1-x}As$ shows two-mode behavior in the first order Raman scattering, which are LO and TO phonons corresponding to both InAs and GaAs binary parent materials, and the frequency positions depend on the In composition (x).[20-22] Fig. 3 shows Raman spectra of the $In_{0.53}Ga_{0.47}As$ epi-layers with different buffer layers. For both samples of A and B, two strong peaks located at 226 cm^{-1} and 267 cm^{-1} occur, corresponding to TO phonon modes of InAs and LO phonon modes of GaAs, respectively. However, in the Raman spectra we can not clearly observe the peaks of LO_{InAs} and TO_{GaAs}, which are around 244 cm^{-1} and 254 cm^{-1}, respectively. The LO_{InAs} and TO_{GaAs} modes are related to disorder-activated lattice vibrations which are supposed to exist in $In_{0.53}Ga_{0.47}As$ materials.[22] The Raman results indicate high-crystallinity of the $In_{0.53}Ga_{0.47}As$ epitaxial films obviously.

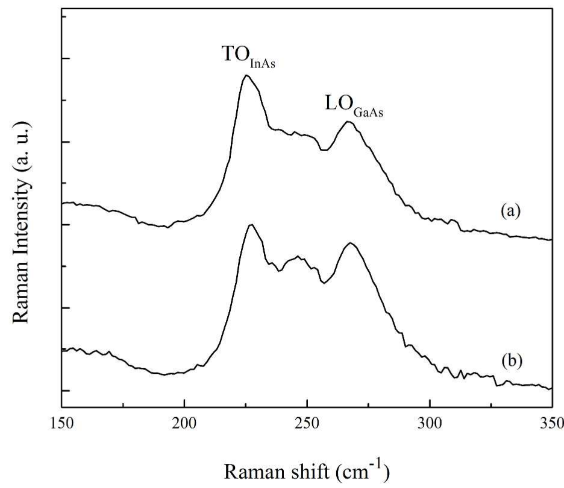

Fig. 3 Raman spectra of sample A (a) and B (b), respectively.

The evaluations of the stress of the $In_xGa_{1-x}As$ epi-layers are made from a frequency shift of the GaAs-like LO phonon.[23] The GaAs-like LO phonon frequency Ω_{LO} is blue-shifted for compressive layers (ε<0), between the values of the relaxed and fully strained material. The shifts are proportional to the residual strain ε, and depend on the In composition and the growth orientation,[24]

$$\Delta\Omega_{LO(111)} = \Omega_{uns}[(\widetilde{K}_{11} + 2\widetilde{K}_{12})(2-\Gamma) - 4\widetilde{K}_{11}(1+\Gamma)]\varepsilon / 6 \quad (1)$$

where

$$\Gamma_{(111)} = (2C_{11} + 4C_{12} - 4C_{44})/(C_{11} + 2C_{12} + 4C_{44}) \quad (2)$$

Γ is the inverse of the Poisson ratio, which is dependent on the orientation, C_{ij} is the elastic constants, $\widetilde{K}_{ij}$ are the phonon deformation potentials of the $In_{0.53}Ga_{0.47}As$ layer. The C_{ij} and $\widetilde{K}_{ij}$ have been linearly interpolated from data[25] for InAs and GaAs. The phonon frequency of the unstrained material has been determined on completely relaxed samples, with the result Ω_{uns}=292.2-35.72x-14.82x^2 at 300 K.[24]

CrystEngComm Accepted Manuscript

Using the measured results $\Delta\Omega_{LO}$ and Eq. (1)-(2), it can be obtained that the stress of the $In_{0.53}Ga_{0.47}As$ epi-layes in samples A and B is -481.56 MPa and -371.29 MPa, respectively. This means the residual stress in the $In_{0.53}Ga_{0.47}As$ layers is compressive stress. The stress in epi-layers mainly caused by the lattice mismatch between the $In_{0.53}Ga_{0.47}As$ epi-layer and Si substrate is decreased by using the buffer layers. And the residual stress of the sample B is lower than the sample A. Therefore, crystalline quality of the $In_{0.53}Ga_{0.47}As$ epi-layers can be improved by using the low temperature buffer layer with in-situ annealing growth on the Si substrate.

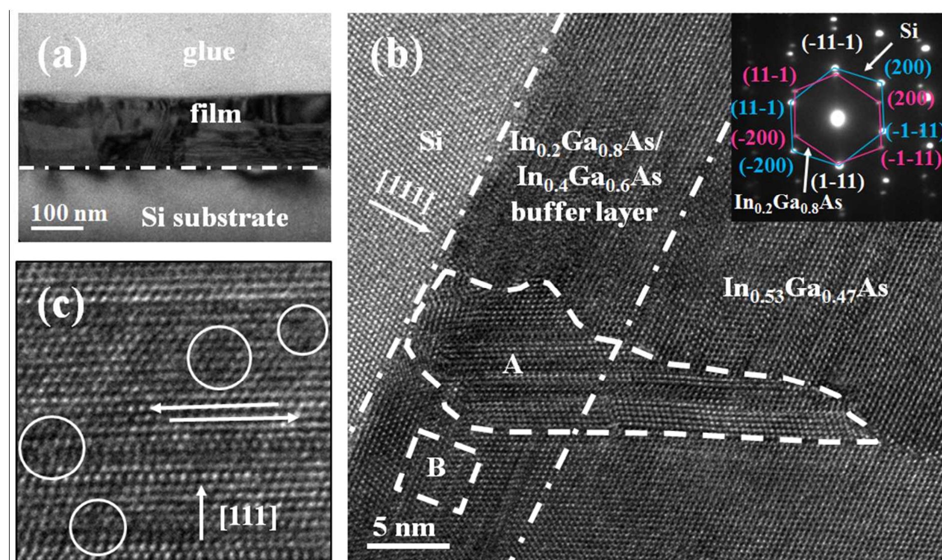

Fig. 4 Cross-sectional TEM images for sample A grown on Si substrate. (a) a bright field cross-sectional TEM image at low magnification for the interface between the $In_{0.53}Ga_{0.47}As$ epitaxial layer and Si under the two-beam diffraction condition of g=[02-2], (b) its corresponding high-resolution cross-sectional TEM micrograph around the interface, the inset is SAED image of the interface between the buffer layer and Si substrate, in which the solid lines marked in blue and pink are corresponding to diffraction planes of Si and buffer layer, respectively, and (c) magnified view of the $In_{0.2}Ga_{0.8}As/In_{0.4}Ga_{0.6}As$ buffer layers.

Cross-sectional TEM investigation was carried out to investigate the structure of $In_{0.53}Ga_{0.47}As$ films grown on Si (111) substrate. Fig. 4(a) is a bright filed cross-sectional TEM image of sample A under the two-beam diffraction condition of g = [02-2], where misfit dislocation and threading dislocation can be observed from their sharp contrast against the matrix, and the interface between the $In_{0.2}Ga_{0.8}As/In_{0.4}Ga_{0.6}As$ buffer layers and Si substrate can also be clearly observed, as illustrated by the white dash-dot line. The buffer layers contain a much higher density of dislocations, which are along the interface. It can also be easily found that a high density of misfit dislocations occur in the vicinity of the interface between buffer layer and $In_{0.53}Ga_{0.47}As$ epi-layer. From the selective area electron diffraction (SAED) of the interface, we obtain the epitaxial relationship between the buffer layer and Si

CrystEngComm Accepted Manuscript

substrate, which is $In_{0.2}Ga_{0.8}As$ (111) ‖ Si (111), as shown in the insert of Fig. 4(b). Fig. 4(b) shows that thickness of the $In_{0.2}Ga_{0.8}As/In_{0.4}Ga_{0.6}As$ buffer layers is about 12 nm, as illustrated by two white dash-dot lines. Furthermore, the compressive stress derived from the lattice mismatch can result in stacking faults along the epitaxial direction, which ultimately extend to the $In_{0.53}Ga_{0.47}As$ epilayer, as shown by dash-line segment A in Fig. 4(b). As the epi-layer thickness gradually increases, the stacking faults are greatly decreased and even annihilated toward the epitaxial layer. In addition, the stacking faults have also been observed parallel to the direction of the interface at the buffer layer, as shown in Fig. 4(c), which its magnified view of the dash-line segment B of Fig. 4(b). Circles in Fig. 4(c) show the defects inside the buffer layer, and the high density of the defects in the buffer is detrimental to the subsequent growth of the $In_{0.53}Ga_{0.47}As$ epitaxial layer.

Due to lattice mismatch between $In_{0.53}Ga_{0.47}As$ and Si, the $In_{0.53}Ga_{0.47}As$ lattice is subjected to large compression strain from the Si lattice, leading to substantial mismatch stress at the $In_{0.53}Ga_{0.47}As$/buffer layer and buffer layer/Si interface during epitaxial growth. In order to release the mismatch stress, misfit dislocations are generated at the buffer layer/Si and $In_{0.53}Ga_{0.47}As$/buffer layer interfaces. As the film thickness gradually increases, these interfacial misfit dislocations propagate and stretch upwards, resulting in the formation of threading dislocations and stacking fault. However, with increasing thickness of the epitaxial $In_{0.53}Ga_{0.47}As$ film, the compression strain inside the film is gradually reduced and the threading dislocations can also be annihilated, as illustrated in Fig. 4(b).

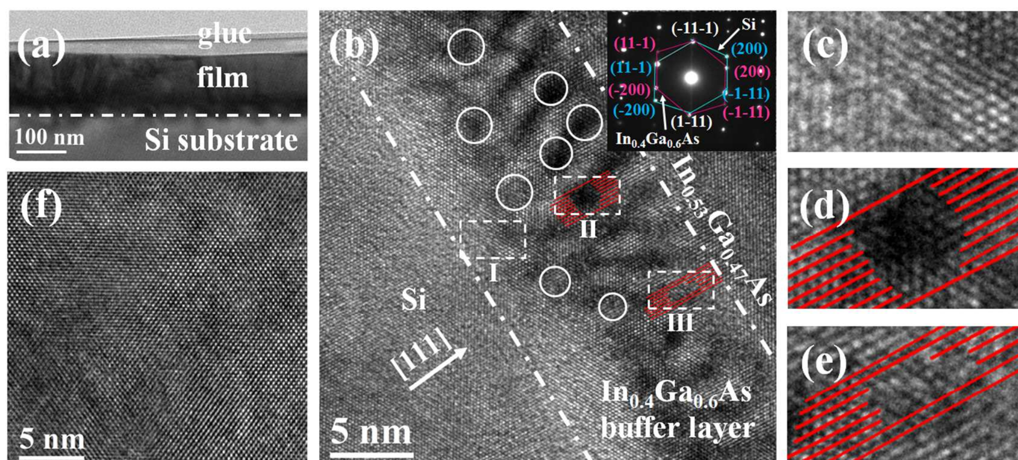

Fig. 5 Cross-sectional TEM images for sample B grown on Si substrate. (a) a bright field cross-sectional TEM image at low magnification under the two-beam diffraction condition of g=[02-2], (b) high-resolution cross-sectional TEM micrograph around the interface, the inset is SAED image of the interface between the $In_{0.4}Ga_{0.6}As$ buffer layer and Si substrate, in which the solid lines marked in blue and pink are corresponding to diffraction planes of Si and $In_{0.4}Ga_{0.6}As$, respectively, (c-e) magnified view of the $In_{0.4}Ga_{0.6}As$ buffer layer in region I, II and III, respectively, and (f) high-resolution cross-sectional TEM micrograph of $In_{0.53}Ga_{0.47}As$ epilayer.

CrystEngComm Accepted Manuscript

Fig. 5 shows cross-sectional TEM images of sample B in which a single layer of $In_{0.4}Ga_{0.6}As$ buffer layer is adopted. From Fig. 5(a) we can notice that the interface between Si (111) substrate and epi-layer is very abrupt. Fig. 5(b) is the typical high-resolution cross-sectional TEM image of sample B, although a high density of screw and edge dislocations is found in the $In_{0.4}Ga_{0.6}As$ buffer layer, as illustrated by the circles, no threading dislocation occurs in the buffer layer. In addition, the epitaxial relationship of $In_{0.4}Ga_{0.6}As$ (111) || Si (111) is distinctly illustrated from SAED patterns, as shown in Fig. 5(b) inset. In order to study the defect distribution in the buffer layer in details, three typical regions are selected and marked as I, II, and III in various positions of the buffer layer, as shown in Fig. 5(b). The magnified corresponding images are shown in Fig. 5(c)-(e), respectively. For region I, due to the lattice misfit of 7.08 % between $In_{0.4}Ga_{0.6}As$ and Si, high density of defects especially lattice distortion arose in the vicinity of $In_{0.4}Ga_{0.6}As$/Si interface. On the other hand, Fig. 5(d) and 5(e) display high levels of stacking faults and dislocations. One of the most significant phenomena we have to pay attention is that although many defects such as lattice distortions and stacking faults can be found inside the $In_{0.4}Ga_{0.6}As$ buffer layer, the interface of $In_{0.4}Ga_{0.6}As/In_{0.53}Ga_{0.47}As$ is very abrupt with lower threading dislocation density, resulting in the high-crystallinity $In_{0.53}Ga_{0.47}As$ epitaxial film. We can note that the $In_{0.53}Ga_{0.47}As$ epitaxial film is of a high degree of structural perfection, as shown in Fig. 5(f).

We have tried to understand how the single $In_{0.4}Ga_{0.6}As$ buffer layer can efficiently release misfit strain and trap dislocations by using low temperature growth and in-situ annealing. It has been reported that low-temperature buffer layer will provide low energy sites for the nucleation of dislocations and point defects, which, on the one hand, effectively prevents the propagation of these defects into the subsequent epi-layer and, on the other hand, releases the misfit strain between the substrate and epi-layer.[26, 27] Moreover, the atoms will rearrange within the buffer layer by the in-situ annealing process, which helps to release the misfit strain caused by lattice mismatch between the substrate and the subsequent $In_{0.53}Ga_{0.47}As$ epi-layer. In this paper, the low-temperature single $In_{0.4}Ga_{0.6}As$ buffer layer with in-situ annealing in this work will trap threading dislocation. Furthermore, it will introduce high density of defects within the $In_{0.4}Ga_{0.6}As$ buffer layer to reduce the lattice misfit strain. In other words, although a very high density of point defects and dislocations are generated within the $In_{0.4}Ga_{0.6}As$ buffer layer, the defects are confined in the $In_{0.4}Ga_{0.6}As$ buffer layer, without extending to the subsequently grown $In_{0.53}Ga_{0.47}As$ epi-layer.

4. Conclusions

To conclude, we have studied the structural properties of $In_{0.53}Ga_{0.47}As$ films grown on Si (111) substrates with the composition-graded $In_{0.2}Ga_{0.8}As/In_{0.4}Ga_{0.6}As$ buffer layers (sample A) and a single $In_{0.4}Ga_{0.6}As$ buffer layer (sample B), respectively. The FWHMs from XRCs are about 595.56 and 556.41 arcsec for the as-grown two $In_{0.53}Ga_{0.47}As$ (111) epi-layers, respectively, indicating that the crystalline quality of as-grown $In_{0.53}Ga_{0.47}As$ epi-layers grown on Si substrate by

CrystEngComm Accepted Manuscript

using low-temperature $In_{0.4}Ga_{0.6}As$ buffer layer with in-situ annealing is better than that by using composition-graded $In_{0.2}Ga_{0.8}As/In_{0.4}Ga_{0.6}As$ buffer layers. RSMs have been used to study the strain relaxation value of as-grown $In_{0.53}Ga_{0.47}As$ films with two different buffer layers. The relaxation value of as-grown $In_{0.53}Ga_{0.47}As$ epi-layers for sample A and sample B are 90.23 % and 97.16 %, respectively. Furthermore, the residual stresses derived from Raman spectra are calculated to be -481.56 MPa and -371.29 MPa for sample A and B, respectively. These results illustrate that the mismatch strain inside the $In_{0.53}Ga_{0.47}As$ layer can be effectively released by a single $In_{0.4}Ga_{0.6}As$ buffer layer compared with the composition-graded buffer layer.

From TEM characterisation, we can further understand the strain relaxation mechanism and dislocation distribution of the buffer layers and epi-layers grown on Si substrate. For sample A, misfit dislocations are generated at the interfaces. As the film thickness gradually increases, these interfacial misfit dislocations propagate and stretch upwards, resulting in the formation of threading dislocations and stacking fault. For sample B, defects of the $In_{0.53}Ga_{0.47}As$ epilayer are confined into the low-temperature single $In_{0.4}Ga_{0.6}As$ buffer layer, without extending to the subsequent grown $In_{0.53}Ga_{0.47}As$ epi-layer. Furthermore, the atoms will rearrange within the buffer layer through the annealing process, which is favorable for the subsequent epitaxy of the $In_{0.53}Ga_{0.47}As$ layer. This achievement represents a simple but effective approach to achieve high-crystallinity $In_{0.53}Ga_{0.47}As$ film on the Si substrates.

Acknowledgements

The authors gratefully acknowledge financial support from the National Science Fund for Excellent Young Scholars of China (No. 51422203), National Science Foundation of China (No. 51372001), National Key Basic Research Project of China (973 Project), Excellent Youth Foundation of Guangdong Scientific Committee (No. S2013050013882), Key Project in Science and Technology of Guangdong Province (No. 2011A080801018), and the Fundamental Research Funds for the Central Universities (x2c1-D2142w). Fangliang Gao and Lei Wen contributed equally to this work.

References

1. J. M. Zahler, K. Tanabe, C. Ladous, T. Pinnington, F. D. Newman and H. A. Atwater, *Appl. Phys. Lett.*, 2007, **91**(1), 012108-3.
2. N. N. Ledentsov, V. A. Shchukin, T. Kettler, K. Posilovic, D. Bimberg, L. Y. Karachinsky, A. Y. Gladyshev, M. V. Maximov, I. I. Novikov, Y. M. Shernyakov, A. E. Zhukov, V. M. Ustinov and A. R. Kovsh, *J. Cryst. Growth*, 2007, **301-302**, 914-922.
3. Y. Kang, Y. H. Lo, M. Bitter, S. Kristjansson, Z. Pan and A. Pauchard, *Appl. Phys. Lett.*, 2004, **85**(10), 1668-1670.
4. N. A. Papanicolaou, G. W. Anderson, A. A. Iliadis and A. Christou, *J. Electron. Mater.*, 1993, **22**(2), 201-206.
5. G. Q. Miao, T. M. Zhang, Z. W. Zhang and Y. X. Jin, *CrystEngComm*, 2013, **15**(42), 8461-8464.

CrystEngComm Accepted Manuscript

6. E. A. Chagarov and A. C. Kummel, *Surf. Sci.*, 2009, **603**(21), 3191-3200.
7. J. M. Kuo, Y. C. Wang, J. S. Weiner, D. Sivco, A. Y. Cho and Y. K. Chen, *J. Cryst. Growth*, 2001, **227-228**, 362-365.
8. T.-H. Chiang, S.-Y. Wu, T.-S. Huang, C.-H. Hsu, J. Kwo and M. Hong, *CrystEngComm*, 2014, DOI: 10.1039/C4CE00734D, *In Press*.
9. S. Kim, M. Yokoyama, N. Taoka, R. Iida, S. Lee, R. Nakane, Y. Urabe, N. Miyata, T. Yasuda, H. Yamada, N. Fukuhara, M. Hata, M. Takenaka and S. Takagi, *Appl. Phys. Express*, 2012, **5**(1), 014201-3.
10. H. Kawanami, *Sol. Energy Mater. Sol. Cells.*, 2001, **66**(1-4), 479-486.
11. Z. Mi and Y. L. Chang, *J. Nanophotonics*, 2009, **3**, 031602-031619.
12. T. Y. Wang, S. L. Ou, R. H. Horng and D. S. Wuu, *CrystEngComm*, 2014, **16**(25), 5724-5731.
13. Y.-T. Sun, H. Kataria, W. Metaferia and S. Lourdudoss, *CrystEngComm*, 2014, DOI: 10.1039/C4CE00844H, *In Press*.
14. M. C. Tseng, R. H. Horng, D. S. Wuu and M. D. Yang, *IEEE. J. Quantum. Elect.*, 2011, **47**(11), 1434-1442.
15. H. Lin, Y. J. Huo, Y. W. Rong, R. Chen, T. I. Kamins and J. S. Harris, *J. Cryst. Growth*, 2011, **323**(1), 17-20.
16. M. Fatemi and R. E. Stahlbush, *Appl. Phys. Lett.*, 1991, **58**(8), 825-827.
17. S. M. Sze and K. K. Ng, *Physics of Semiconductor Devices*, John Wiley & Sons, New Jersey, 2006.
18. M. W. Dashiell, H. Ehsani, P. C. Sander, F. D. Newman, C. A. Wang, Z. A. Shellenbarger, D. Donetski, N. Gu and S. Anikeev, *Sol. Energy Mater. Sol. Cells.*, 2008, **92**(9), 1003-1010.
19. M. R. Islam, P. Verma, M. Yamada, M. Tatsumi and K. Kinoshita, *Jpn. J. Appl. Phys.*, 2002, **41**(2B), 991-995.
20. J. P. Estrera, P. D. Stevens, R. Glosser, W. M. Duncan, Y. C. Kao, H. Y. Liu and E. A. Beam III, *Appl. Phys. Lett.*, 1992, **61**(16), 1927-1929.
21. J. Groenen, G. Landa, R. Carles, P. S. Pizani and M. Gendry, *J. Appl. Phys.*, 1997, **82**(2), 803-809.
22. T. P. Pearsall, R. Carles and J. C. Portal, *Appl. Phys. Lett.*, 1983, **42**(5), 436-438.
23. T. M. Zhang, G. Q. Miao, Y. X. Jin, S. Z. Yu, H. Jiang, Z. M. Li and H. Song, *J. Alloy. Compd.*, 2009, **472**(1-2), 587-590.
24. F. Calle, A. L. Alvarez, A. Sacedon, E. Calleja and E. Munoz, *Phys. Status Solidi A*, 1995, **152**(1), 201-209.
25. S. Adachi, *J. Appl. Phys.*, 1982, **53**(12), 8775-8792.
26. Y. H. Luo, J. Wan, R. L. Forrest, J. L. Liu, G. Jin, M. S. Goorsky and K. L. Wang, *Appl. Phys. Lett.*, 2001, **78**(4), 454-456.
27. F. L. Gao and G. Q. Li, *Appl. Phys. Lett.*, 2014, **104**(4), 042104-5.

CrystEngComm Accepted Manuscript